I&EC research
Industrial & Engineering Chemistry Research

Article

pubs.acs.org/IECR

Promotion Effect of Alkali Metal Hydroxides on Polymer-Stabilized Pd Nanoparticles for Selective Hydrogenation of C−C Triple Bonds in Alkynols

Linda Zh. Nikoshvili,*[,†] Alexey V. Bykov,[†] Tatiana E. Khudyakova,[†] Thomas LaGrange,[‡] Florent Héroguel,[§] Jeremy S. Luterbacher,[§] Valentina G. Matveeva,[†] Esther M. Sulman,[†] Paul J. Dyson,[∥] and Lioubov Kiwi-Minsker*[,∥,⊥]

[†]Department of Biotechnology and Chemistry, Tver Technical University, A. Nikitina Street, 22, 170026, Tver, Russia
[‡]Interdisciplinary Centre for Electron Microscopy (CIME), [§]Laboratory of Sustainable and Catalytic Processing, and [∥]Laboratory of Organometallic and Medical Chemistry, Ecole Polytechnique Fédérale de Lausanne (EPFL), CH-1015, Lausanne, Switzerland
[⊥]Tver State University, Regional Technological Center, Zhelyabova Street, 33, 170100, Tver, Russia

Supporting Information

ABSTRACT: Postimpregnation of Pd nanoparticles (NPs) stabilized within hyper-cross-linked polystyrene with sodium or potassium hydroxides of optimal concentration was found to significantly increase the catalytic activity for the partial hydrogenation of the C−C triple bond in 2-methyl-3-butyn-2-ol at ambient hydrogen pressure. The alkali metal hydroxide accelerates the transformation of the residual Pd(II) salt into Pd(0) NPs and diminishes the reaction induction period. In addition, the selectivity to the desired 2-methyl-3-buten-2-ol increases with the K- and Na-doped catalysts from 97.0 up to 99.5%. This effect was assigned to interactions of the alkali metal ions with the Pd NPs surfaces resulting in the sites' separation and a change of reactants adsorption.

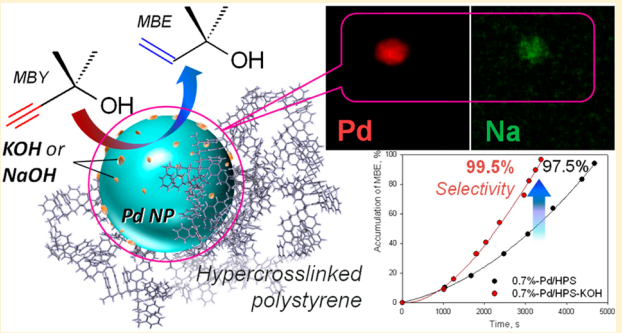

1. INTRODUCTION

Pd-catalyzed selective hydrogenations of the carbon−carbon triple bond in alkynols is an important reaction in the production of fine chemicals such as fragrances (linalool, terpineol, geraniol, citral, etc.), pharmaceuticals, and fat-soluble vitamins (e.g., E, K).[1,2] Industrial alkynol hydrogenation is usually carried out as a 3-phase reaction using the Lindlar catalyst ($Pd/CaCO_3$ doped with lead acetate) in the presence of quinolone, employed as liquid-phase modifier. This system delivers a selectivity around 95% at close to 100% conversion.[1,3,4] However, the modifiers can contaminate the target product, which is unacceptable to the pharmaceutical and food industries.

Despite numerous achievements in the development of alternative catalysts to the industrial Lindlar catalytic process,[4] attaining high selectivity with reasonable activity/stability (especially in the case of alkynols containing terminal C−C triple bonds) remains challenging and requires careful selection of the catalyst and optimization of the reaction conditions.

There are several ways to improve catalyst efficiency in hydrogenations of triple bonds, for example, adjusting the size and morphology of Pd nanoparticles (NPs),[5] with small Pd NPs known to be selective due to the absence of a β-hydride phase,[6] and/or the addition of a second metal to the Pd NP system. There are two main ways to improve selectivity, also involving addition of a second metal to form bimetallic alloyed NPs and/or the addition of promoters, surface dopants, or modifiers. It is noteworthy that "catalytic poisons" such as Pb and Sn, and other metals such as Na, K, Zn, Ag, Au, etc., may be used. For example, it was shown that the addition of Ag results in the formation of alloyed Ag−Pd NPs and a selectivity of 96% for the partially hydrogenated product of dehydroisophytol (cf. Pd NPs which exhibit a selectivity of 78%).[7]

Alkali metal cations are known promoters of Pd-containing hydrogenation catalysts,[8−15] often incorporated by postimpregnation of Pd-catalyst with aqueous solutions containing alkali metal cations with subsequent reduction in a hydrogen atmosphere.[8−10] Cho et al. have shown that postimpregnation provides enhanced catalytic activity of the target product in the hydrogenation of biphenol over Pd/C in comparison to preimpregnated and coimpregnated catalysts. It was suggested

Special Issue: Tapio Salmi Festschrift

Received: April 17, 2017
Revised: July 19, 2017
Accepted: July 21, 2017
Published: July 21, 2017

DOI: 10.1021/acs.iecr.7b01612
Ind. Eng. Chem. Res. XXXX, XXX, XXX−XXX

Table 1. MBY Hydrogenation over the 0.7%-Pd/MN100 Catalysts[a]

N	catalyst	modifier	$S_{MBE} \pm 0.5$, % (X_{MBY} = 95%)	$R \pm 0.1$, $mol_{MBY} \cdot mol^{-1}_{Pd} \cdot s^{-1}$
1	0.7%-Pd/MN100	none	97.5	4.2
2	0.7%-Pd/MN100-R	none	95.0	4.1
3	0.7%-Pd/MN100-w	treated with H_2O	97.0	3.7
4	0.7%-Pd/MN100-Na	NaOH, 0.5 mol/L	99.0	5.9
5	0.7%-Pd/MN100-K-1	KOH, 0.1 mol/L	99.5	3.6
6	0.7%-Pd/MN100-K-2	KOH, 0.25 mol/L	98.5	4.6
7	0.7%-Pd/MN100-K-3 first use	KOH, 0.5 mol/L	99.0	7.1
8	0.7%-Pd/MN100-K-3 first use without *in situ* reduction		99.0	5.2
9	0.7%-Pd/MN100-K-3 second use		98.0	3.8
10	0.7%-Pd/MN100-K-3 modified additionally after the first use		99.0	3.3
11	0.7%-Pd/MN100-R-K-3		98.5	2.0
12	0.7%-Pd/MN100-K-3-R		94.5	6.0
13	0.7%-Pd/MN100-K-4	KOH, 1.0 mol/L	98.5	4.3

[a]Reaction conditions: toluene (30 mL), 90 °C, MBY concentration 0.6 mol/L (1.5 g), Pd concentration 4.4×10^{-5} mol/L (0.02 g of the catalyst).

that postimpregnation results in the alkali metal being located in the vicinity of the catalytically active Pd NPs.[10]

Pellegrini et al. demonstrate a promotion effect of K_2CO_3 on a $Pd/SiO_2-Al_2O_3$ catalyst, which leads to the formation of mixed K/Pd-oxides even at low potassium content.[8] It should be emphasized that the formation of a mixed oxide phase is possible only at high temperatures (>500 °C).[16] Alkali metal salts can also influence the mobility of Pd NPs on solid supports, thus preventing sintering during thermal treatments.[8,10] It is noteworthy that in contrast to the results of Pellegrini et al.,[8] Jia et al.[9] did not find any mixed Pd/K-containing species. However, K-containing species either on the Pd NPs, in the form of islands, or at the interface between Pd and the support were not excluded.[9] This so-called "geometric effect" of alkali metal ions may help preserve catalytically active Pd NPs from sintering during catalyst reduction at high temperatures. However, due to the geometric effect, alkali metal ions, especially at high loadings, may decrease the catalytic activity by blocking active sites.[10]

There are also other reasons of adding alkali metal salts to Pd-containing catalysts, for example, they help to avoid HCl accumulation during hydrodechlorination processes.[12−14] In the case of hydrodechlorination of chlorobenzene, Aramendía et al. have shown that the presence of Na^+ ions in the vicinity of the Pd NPs facilitates chlorobenzene adsorption by capturing the chloride with the formation of NaCl.[12] However, only highly dispersed palladium can benefit from the addition of NaOH.[13]

Herein, we present the beneficial effects of postimpregnation of Pd NPs catalyst based on hyper-cross-linked polystyrene (HPS) by aqueous solutions of alkali metal hydroxides (NaOH and KOH). The Pd/HPS catalyst was previously shown to be promising catalyst for the partial hydrogenation of triple C−C bonds in alkynols.[17−19]

The nature of the Pd precursor and the type of HPS (functionalized or without any functional groups) strongly influences the activity of HPS-based catalysts. In our previous work, MN100-type HPS impregnated with $PdCl_2(CH_3CN)_2$ and reduced *in situ* with hydrogen was shown to be the most efficient catalyst leading to a selectivity of ∼98%, with reasonable activity, in the partial hydrogenation of 2-methyl-3-butyn-2-ol (MBY).[17] However, independent of the nature of the precursor, the catalysts based on the MN100 support show an induction period in spite of an *in situ* catalyst activation procedure. In the present study we address the question of the induction period and the influence of alkali metal hydroxides on this phenomenon in order to optimize the catalytic efficiency (activity and selectivity) of the Pd/HPS catalysts.

2. EXPERIMENTAL SECTION

Materials. HPS Macronet MN100 (Purolite Int., United Kingdom) was washed with distilled water and acetone and dried under vacuum as described elsewhere.[20] 2-Methyl-3-butyn-2-ol (MBY, >99%), 2-methyl-3-buten-2-ol (MBE, >97%), 2-methyl-2-butanol (MBA, >96%), bis(acetonitrile)-palladium(II)chloride ($PdCl_2(CH_3CN)_2$, >99%), tetrahydrofuran (THF, ≥99.9%), toluene (99.8%), potassium hydroxide (KOH, ≥85%), sodium carbonate (Na_2CO_3, ≥99.5%) and sodium hydroxide (NaOH, ≥98%) were obtained from Sigma-Aldrich. All chemicals were used as received. Distilled water was purified with an Elsi-Aqua water purification system.

Catalyst Synthesis. Pd/MN100 catalyst was synthesized via the conventional wet-impregnation method according to the procedure described elsewhere.[20] In a typical experiment, 3 g of pretreated, dried, and crushed (<63 μm) granules of HPS were impregnated with 9 mL of the $PdCl_2(CH_3CN)_2$ THF solution (concentration 0.022 mol/L). The Pd-containing polymer was dried at 70 °C, treated with 8.5 mL of Na_2CO_3 aqueous solution (concentration 0.08 mol/L) and dried until a constant weight was achieved. It was expected that such a treatment would lead to hydrolysis of $PdCl_2(CH_3CN)_2$ and precipitation of PdO inside the HPS cavities. The catalyst was washed with distilled water until a pH of 7 was reached and then dried at 70 °C. In this way the catalyst with metal loading of 0.7 wt % was obtained (designated as 0.7%-Pd/MN100 and used as a reference). This catalyst was also reduced in hydrogen at a H_2 flow rate of 100 mL/min and a temperature of 300 °C for 2 h (designated as 0.7%-Pd/MN100-R).

The obtained catalysts (i.e., without and with H_2 reduction) were modified with NaOH or KOH prior to catalysis. In a typical experiment, 0.02 g of 0.7%-Pd/MN100 or 0.7%-Pd/MN100-R was impregnated with 0.09 mL of alkaline hydroxide solution. In the case of NaOH, a concentration of 0.5 mol/L was used (catalyst designated as 0.7%-Pd/MN100-Na), while in the case of KOH concentrations of 0.1, 0.25, 0.5, and 1 mol/L were used (catalysts designated as 0.7%-Pd/MN100-K-1, 0.7%-Pd/MN100-K-2, 0.7%-Pd/MN100-K-3, and 0.7%-Pd/MN100-K-4, respectively; see Table 1). After modification all the catalysts were dried at 75 °C for 20 h.

DOI: 10.1021/acs.iecr.7b01612
Ind. Eng. Chem. Res. XXXX, XXX, XXX−XXX

The 0.7%-Pd/MN100 catalyst was also treated with distilled water (designated as 0.7%-Pd/MN100-w) according to the procedure described above in order to reveal the influence of alkali metal cation.

The possibility of gas-phase reduction of the catalyst modified with 0.5 mol/L aqueous solution of KOH (designated as 0.7%-Pd/MN100-K-3-R) was also investigated.

The general scheme of the used treatments of the 0.7%-Pd/MN100 catalysts is presented in Figure 1.

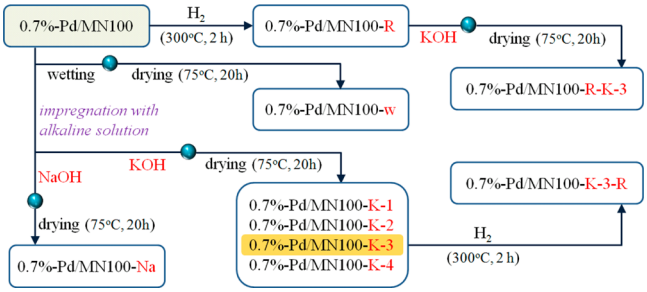

Figure 1. Modification and reduction of 0.7%-Pd/MN100 catalysts.

Additionally, the *in situ* activation by hydrogen during 60 min was applied to all catalysts before testing.

Catalyst Testing: Setup, Procedure, and Analytics. Testing of the catalysts in the selective hydrogenation of MBY to MBE (Figure 2) was performed at 90 °C in a 60 mL isothermal glass batch reactor connected to a gasometrical buret for *online* monitoring of hydrogen consumption, and installed in a shaker for vigorous mixing (more than 800 two-sided shaking per minute), which excludes external diffusion limitations.[18] The internal diffusion limitations were also excluded via powdering of HPS to <63 μm.[18,19] Toluene was used as a solvent. A recirculating bath (LOIP LT 100, Saint-Petersburg, Russia) was used to stabilize the reaction temperature within ±1 °C using water as the thermal medium. The choice of solvent and reaction temperature was based on previous studies.[18,19]

At the beginning of each experiment, the temperature was set to 90 °C, and allowed to stabilize (ca. 30 min). After that the reactor was charged with catalyst (0.02 g) and toluene (15 mL), and hydrogen was then introduced. All catalysts were activated *in situ* during 60 min before the MBY addition (time "zero", t = 0 for the reaction). It is noteworthy that the addition of MBY (0.018 mol) was accompanied by the addition of 15 mL of toluene, so the total volume of liquid phase was 30 mL. A noninvasive liquid sampling system allowed a controlled removal of aliquots (0.1−0.5 mL) from the reactor by the syringe and analyzed via GC−MS (Shimadzu GCMS-QP2010S) equipped with a capillary column HP-1MS (30 m × 0.25 mm i.d., 0.25 μm film thickness). Helium was used as a carrier gas. The concentrations of the substrate/products were determined using an internal standard (diphenylamine) calibration method. Repeated reaction runs with the same catalyst batch delivered concentration values that were reproducible within ±0.5%. The conversion of MBY is defined as

$$X_{MBY}(\%) = \frac{C_{MBY,0} - C_{MBY}}{C_{MBY,0}} 100$$

and selectivity with respect to MBE as the target product, is

$$S_{MBE}(\%) = \frac{C_{MBE}}{C_{MBY,0} - C_{MBY}} 100$$

Catalytic activity was characterized by the rate of MBY concentration calculated in the range of linear dependency X % on time (induction as well as slow-down periods were excluded from the calculation), and designated as R, [$mol_{MBY} \cdot mol^{-1}_{Pd} \cdot s^{-1}$].

$R = (N_{MBY,X2} - N_{MBY,X1}) \times N_{Pd}^{-1} \times (\tau_2 - \tau_1)^{-1}$, where $N_{MBY,X2}$ and $N_{MBY,X1}$ are the numbers of moles of MBY converted at the reaction time τ_2 and τ_1, respectively; N_{Pd} is the total number of moles of Pd participating in the reaction.

Catalyst Characterization. X-ray photoelectron spectroscopy (XPS) data were obtained using Mg K α ($h\nu$ = 1253.6 eV) radiation on an ES-2403 spectrometer (Institute for Analytic Instrumentation of RAS, St. Petersburg, Russia) equipped with energy analyzer PHOIBOS 100-5MCD (SPECS GmbH, Germany) and X-ray source XR-50 (SPECS GmbH, Germany). All data were acquired at an X-ray power of 250 W. Survey spectra were recorded at an energy step of 0.5 eV with an analyzer pass energy of 40 eV. High resolution spectra were recorded at an energy step of 0.05 eV with an analyzer pass energy of 7 eV. Samples were allowed to outgas for 180 min before analysis and were stable during the examination. The data analysis was performed with CasaXPS. The binding energy of C 1s of the HPS was taken as 285.0 eV. The accuracy of identification of binding energies was 0.1 eV.

Pd NPs sizes were evaluated by high-angle annular dark-field scanning transmission electron microscopy (HAADF STEM) using FEI Talos F200S electron microscope working at accelerating voltage of 200 keV. Samples were prepared by embedding the catalyst in epoxy resin (EPON 812, polymerization conditions: 24 h at 333 K) with microtomming (*ca.* 50 nm thick) at ambient temperature. A holey carbon/Cu grid (300 mesh) was used as a sample support. The grid was plasma cleaned (for 5 min) using a Fischione 1070 plasma cleaner operated at a forward power of 10.45 W and 30 sccm gas flow. HAADF STEM measurements were accompanied by the EDX analysis.

DRIFT spectra of CO adsorption were recorded using a high temperature Harrick DRIFT cell on a PerkinElmer Frontier spectrometer equipped with a mercury cadmium telluride detector. The setup enables treatment of the sample with gas flows (He, H_2, CO) and under vacuum from 10 to 500 °C. Spectra were typically collected with 32 scans at a resolution of 4 cm^{-1}.

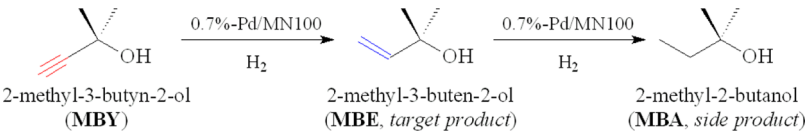

Figure 2. Reaction network of MBY selective hydrogenation to MBE.

DOI: 10.1021/acs.iecr.7b01612
Ind. Eng. Chem. Res. XXXX, XXX, XXX−XXX

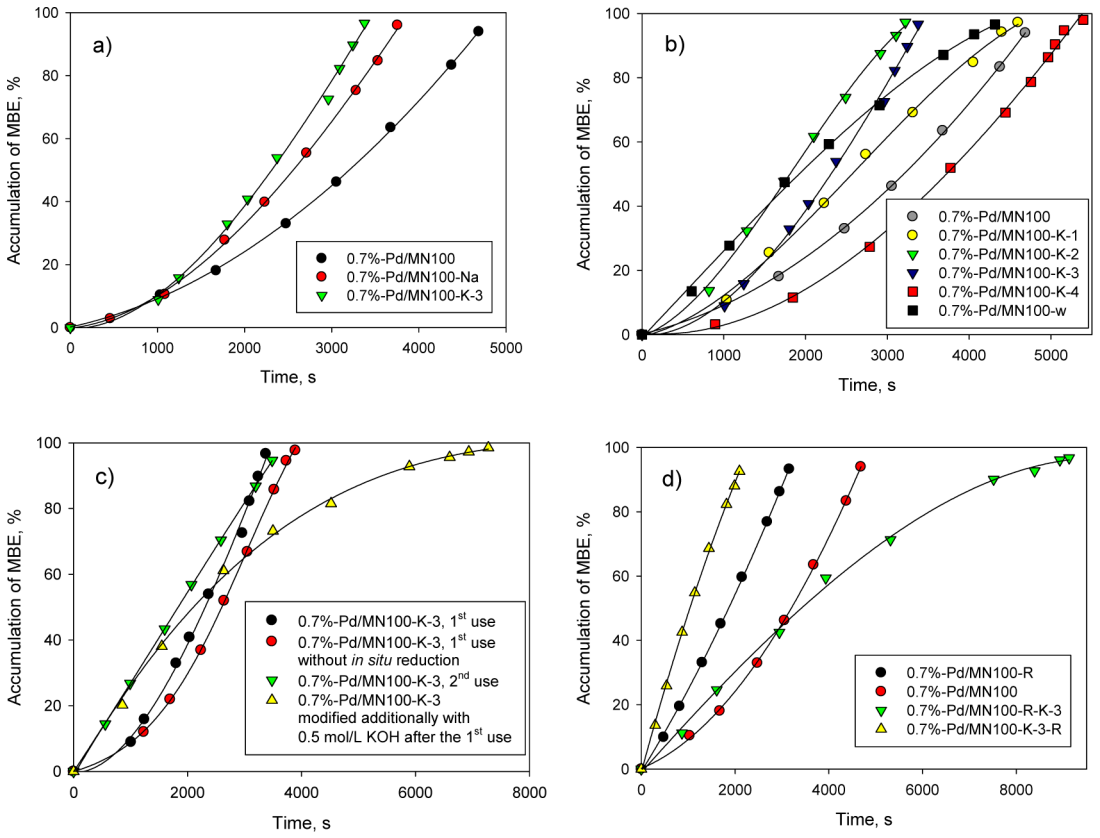

Figure 3. Kinetic curves showing MBE accumulation showing the influence of modifier on the 0.7%-Pd/MN100 catalysts (a), influence of KOH concentration (b), repeated use (c), and influence of gas-phase (hydrogen) reduction (d).

3. RESULTS AND DISCUSSION

3.1. Hydrogenation of MBY. The hydrogenation of MBY using Pd/HPS catalysts (Table 1 and Figure 3) results in the complete conversion of MBY and overhydrogenation of target product (MBE) to MBA. Thus, the reaction was stopped after reaching >99% MBY conversion.

Modification of the reference catalyst 0.7%-Pd/MN100 with 0.5 mol/L aqueous solution of NaOH or KOH results in an increase in selectivity of the partially reduced MBE product (from 97.5% to ca. 99%). A decrease of the induction period accompanied by a ca. 1.4-fold increase of activity (specific transformation rate, R) was also observed (Figure 3a), presumably due to accelerated active site formation (i.e., more facile reduction of residual Pd(II) species in the presence of alkali metal hydroxides) during the *in situ* liquid-phase activation. It is noteworthy that if the *in situ* activation step is excluded (see Figure 3c), a longer induction period is observed, confirming the proposed nature of induction period and the necessity of *in situ* reductive activation.

It should also be noted that the catalyst modified by KOH is more active (the reaction proceeds faster) than the one modified with NaOH (3a). This difference is in agreement with a study by Lamy-Pitara et al. which showed that the activity of a Pt catalyst in the hydrogenation of double bonds depends on the size of the doping cation.[21]

Figure 4 compares the dependency of selectivity vs conversion for the reference catalyst and 0.7%-Pd/MN100-K-3. The higher selectivity was obtained for all MBY conversions up to X = 95% suggesting that doping with KOH changes the reaction network and diminishes MBY overhydrogenation.

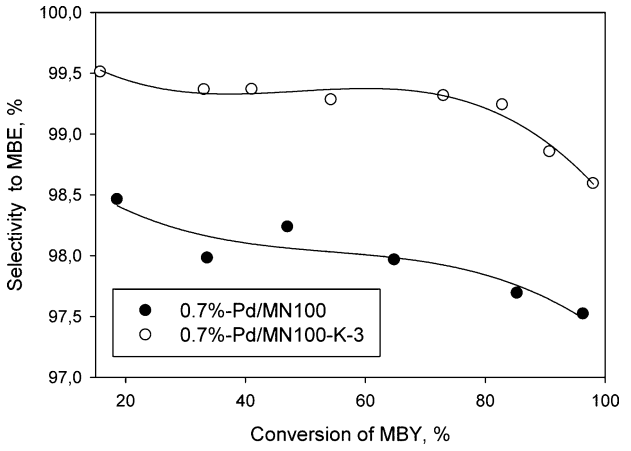

Figure 4. Dependency of selectivity vs conversion of 0.7%-Pd/MN100 and 0.7%-Pd/MN100-K-3 in the partial hydrogenation of MBY.

The influence of the KOH-modifier concentration was studied (Table 1, no. 5–7 and no. 12; Figure 3b) with the concentration of the KOH solution decreasing from 1.0 mol/L stepwise to 0.1 mol/L, revealing an influence on the length of the induction period (Figure 3b; Table 1, no. 3), but with the selectivity to MBE remaining almost constant at 99 ± 0.5%. Only in the case of "zero" concentration of modifier, that is, for 0.7%-Pd/MN100-w (Table 1, no. 3) does the selectivity decrease to 97.0% (i.e., for 0.7%-Pd/MN100-w). Thus, the KOH increases the selectivity and shortens the duration of the induction period as compared to the reference catalyst (see section 3.2). Only at the highest KOH concentration of 1 mol/

DOI: 10.1021/acs.iecr.7b01612
Ind. Eng. Chem. Res. XXXX, XXX, XXX−XXX

L is the induction period the longest of all the catalysts, with a selectivity of ~98.5% at 95% conversion (Table 1, no. 13; Figure 3b). The catalytic activity was observed to increase with the concentration of KOH passing through the maximum at KOH 0.5 mol/L (Table 1, no. 7; Figure 3b). It has previously been suggested that at high concentrations the K^+ ions block the surfaces of the Pd NPs decreasing the reaction rate.[10]

While investigating the adsorption of carbon monoxide and hydrogen on alkali-doped Pd surfaces,[22] it was found that the adsorption energies vary. Thus, the increase in selectivity and activity observed in the partial hydrogenation of MBY using the 0.7%-Pd/MN100-K-3 catalyst (doped by alkali metal at optimized concentration) may be attributed to a change in the adsorption equilibrium of hydrogen and/or the substrate.

The stability of the 0.7%-Pd/MN100-K-3 catalyst was studied by performing repeated reaction runs (see Table 1, no. 7–9; Figure 3c). After the first run the induction period completely disappears, indicating that the induction period is due to the *in situ* reduction of palladium and active site formation. The form of the kinetic curve in the case of second reaction run is similar to that observed for prereduced Pd NP catalysts.[23] After the second run the selectivity of 0.7%-Pd/MN100-K-3 slightly decreases from 99.0% to 98.0% (Table 1, no. 7 and no. 8). Therefore, the catalyst was treated with additional KOH after the first run (Table 1, no. 9) and the selectivity remained at 99.0%, albeit at the expense of the reaction rate (see the kinetic curve of MBE accumulation Figure 3c). The investigation of multiple reuses of the catalyst 0.7%-Pd/MN100-K-3 shows a drop of activity after the first reaction run followed by its stabilization (Figure 5). The selectivity to the desired product MBE remained almost the same 98.5 ± 0.5%.

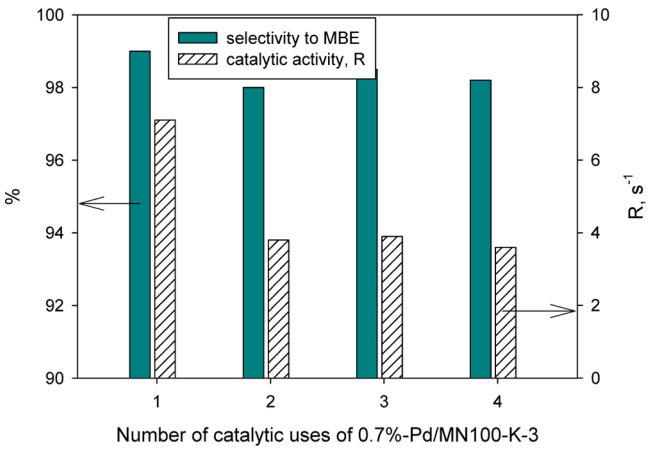

Figure 5. Consecutive reaction runs over the 0.7%-Pd/MN100-K-3.

Reducing 0.7%-Pd/MN100 with hydrogen (Table 1, no. 2) prior to use also resulted in the elimination of induction period (Figure 3d), with the selectivity of the reaction decreasing to 95.0%. This is possibly due to differences in the size of the Pd NPs (see section 3.2, HAADF STEM measurements). The *in situ* liquid-phase reduced Pd NPs have a mean diameter of 4.7 nm following the reaction of MBY, whereas the hydrogen-reduced Pd NPs, performed at 300 °C, are 13.5 nm in diameter (the optimum size for MBY hydrogenation is considered to be 3–5 nm [5]). The selectivity of MBE obtained with the hydrogen-reduced 0.7%-Pd/MN100-R-K-3 catalyst and the reduced KOH-modified 0.7%-Pd/MN100-K-3-R catalyst is the same (94.5%) with the latter catalyst having a ca. 1.5-fold higher activity (Table 1, no. 2 and no. 12).

3.2. Catalyst Characterization. *X-ray Photoelectron Spectroscopy (XPS).* The XPS for the 0.7%-Pd/MN100 reference catalyst (Table 2, Figure S1) reveals the following

Table 2. States of Palladium Found from Modelling of the Pd 3d Band in the XPS Data in Selected Catalysts

	chemical states of Pd on catalyst surface (%)				
			0.7%-Pd/MN100-K-3		
chemical state	0.7%-Pd/MN100	0.7%-Pd/MN100-R	initial	after the *in situ* reduction	after the 1st use
$PdCl_2(CH_3CN)_2$	42	24	59	44	26
$PdCl_2$	21	8	1	6	3
PdO	6	32	28	18	9
Pd^0	7	18	8	11	34
Pd_n clusters	24	18	4	21	28

values of binding energy of Pd $3d_{5/2}$: 337.7 eV (corresponds to $PdCl_2$[24]), 338.6 eV (binding energy of $(CH_3CN)_2PdCl_2$ was found to be equal 338.7 eV), 336.1 eV (small clusters of Pd),[25] 335.0 eV (bulk Pd NPs[24]), and 337.1 eV (corresponds to PdO[24,26]). The $PdCl_2$ is derived from the $PdCl_2(CH_3CN)_2$ precursor. From the XPS analysis of the 0.7%-Pd/MN100-K-3 catalyst (Table 2, Figures S3–S5) there is no evidence for the formation of alkali metal–palladium salts such as K_2PdO_2 or KPdO, which could potentially be formed during the catalyst preparation.[8]

From the presented data (Table 2 and XPS spectra presented in the Supporting Information) it can be seen that post-impregnation of 0.7%-Pd/MN100 with KOH results in a sharp decrease of $PdCl_2$ on the catalyst surface (Figure S1 vs S3) concomitant with the increase of PdO content. Though the rates of reduction of $PdCl_2$ and PdO to both Pd^0 and Pd_n clusters seems to be almost the same, the transformation of $PdCl_2(CH_3CN)_2$ to $PdCl_2$ is slower leading to slower accumulation of palladium chloride for the modified catalyst (0.7%-Pd/MN100-K-3) during the reduction with hydrogen *in situ* and also the subsequent hydrogenation of MBY. This may cause the low concentration of HCl, which is formed as a result of $PdCl_2$ reduction and may inhibit MBY hydrogenation. It can explain the longer induction period in the case of reference sample 0.7%-Pd/MN100 as compared to 0.7%-Pd/MN100-K-3. After the first catalytic run the 0.7%-Pd/MN100-K-3 catalyst contains considerably more Pd NPs (Figure S5), which is also consistent with the absence of the induction period observed during the second run (Figure 3).

It is important to underline that the reduction of the 0.7%-Pd/MN100-K-3 catalyst is more efficient during the hydrogenation of MBY as compared to the initial *in situ* reduction by hydrogen (see Table 2). Recently, it was shown that after the gas-phase reduction of Pd/MN100 catalysts, Pd^{2+} species are observed in the resulting MN100-based samples irrespective of the Pd precursor used.[27] The 0.7%-Pd/MN100-R catalyst, prepared by reduction in hydrogen at 300 °C also contains different Pd species (Table 2, Figure S2), that is, $PdCl_2(CH_3CN)_2$, $PdCl_2$, PdO, Pd_n clusters, and Pd NPs. It is noteworthy that the total percentage of Pd_n clusters and Pd NPs (36%) for the 0.7%-Pd/MN100-R catalyst is similar to the 0.7%-Pd/MN100-K-3 catalyst (32%) after *in situ* reduction.

DOI: 10.1021/acs.iecr.7b01612
Ind. Eng. Chem. Res. XXXX, XXX, XXX–XXX

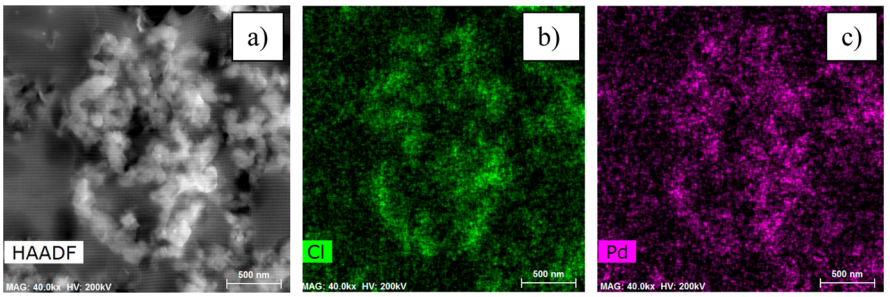

Figure 6. HAADF STEM image (a) and EDX mapping of chlorine (b) and palladium (c) of the 0.7%-Pd/MN100-Na catalyst.

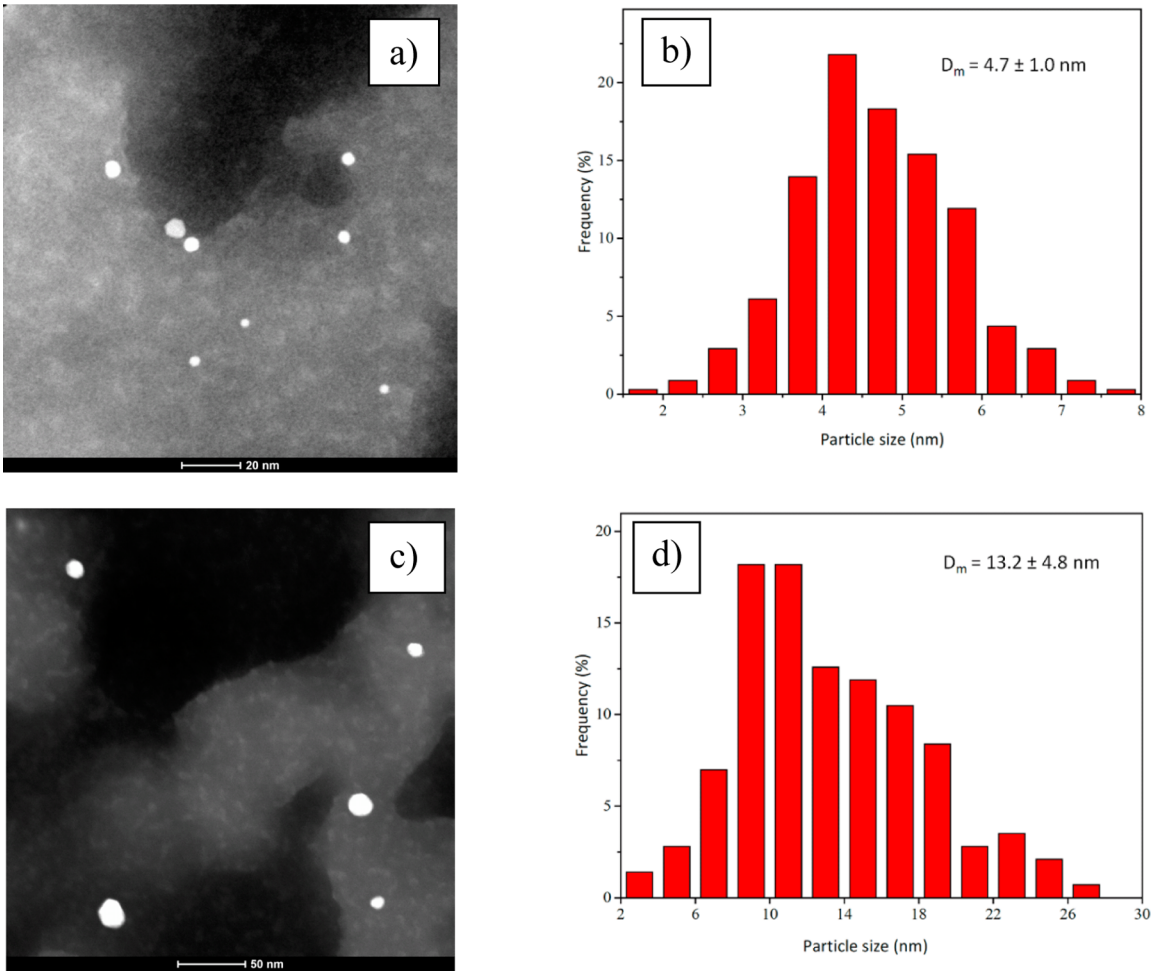

Figure 7. HAADF STEM images and histograms of particle size distributions of the 0.7%-Pd/MN100-Na catalyst after MBY hydrogenation (a,b) and the 0.7%-Pd/MN100-R catalyst (c,d).

It was surprising to find unreduced Pd species, especially in the case of the catalysts treated in hydrogen flow at high temperature. Thus, the reference catalyst 1%-Pd/AC was prepared using $PdCl_2(CH_3CN)_2$ as a precursor and activated carbon (AC) as a support via the same procedure as in the case of MN100. It was found that in the as-synthesized 1%-Pd/AC, $PdCl_2(CH_3CN)_2$ decomposed leaving behind $PdCl_2$ (59.8%) and metallic Pd (34.5%) (Figure S6). After the treatment of this catalyst in H_2 flow at 300 °C for 2 h, only Pd^0 (59.0%) and PdO (41.0%) were found (Figure S7). Formation of PdO could be explained by the interaction of $PdCl_2$ with the −OH containing species of the AC surface being stable under reductive treatment applied.

Therefore, we conclude that MN100 support may stabilize Pd^{2+} species inside the polymeric network probably due to the interaction with the aromatic rings preventing full Pd^{2+} reduction under the H_2 flow.

High-Angle Annular Dark-Field Scanning Transmission Electron Microscopy (HAADF STEM). In the fresh reference 0.7%-Pd/MN100 catalyst and in the alkali metal modified catalysts no Pd NPs were found. EDX mapping of the 0.7%-Pd/MN100-Na clearly shows the presence of molecular dispersion of Pd and Cl in the HPS (Figure 6).

HAADF STEM images and histograms of particle size distributions of the 0.7%-Pd/MN100-Na catalyst recorded after MBY hydrogenation and the 0.7%-Pd/MN100-R catalyst are

DOI: 10.1021/acs.iecr.7b01612
Ind. Eng. Chem. Res. XXXX, XXX, XXX−XXX

shown in Figure 7. For the 0.7%-Pd/MN100-Na catalyst the mean diameter of the Pd NPs is 4.7 ± 1.0 nm (Figure 7a,b), which is essentially the same size as the Pd NPs in a previously reported 0.7%-Pd/MN100 catalyst (4.5 ± 0.9 nm[18]).

In contrast, the 0.7%-Pd/MN100-R catalyst contains Pd NPs with a much larger mean diameter of 13.2 ± 4.8 nm (Figure 7c,d). Despite their larger size they are more efficient catalysts for the hydrogenation of MBY, presumably due to the larger content of Pd(0) as compared to the other catalysts.

To understand the increase of MBE selectivity, the EDX mapping of 0.7%-Pd/MN100-Na catalyst after MBY hydrogenation was carried out. The results are shown in Figure 8 revealing that the surface of the Pd NPs is decorated by sodium.

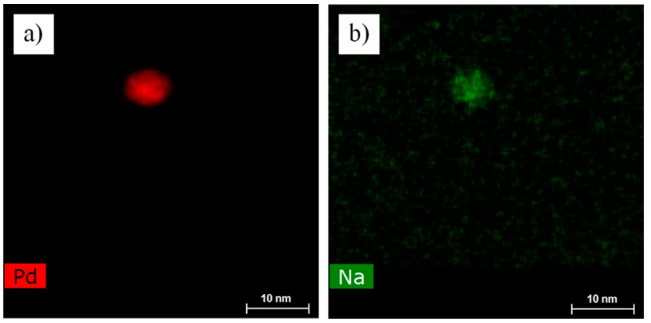

Figure 8. EDX mapping of the 0.7%-Pd/MN100-Na catalyst after MBY hydrogenation: distribution of palladium (a) and sodium (b).

However, Cl is not present on the Pd(0) NPs surface. The alkali metal ions may interact with the Pd NPs resulting in the site separation. This effect can explain the observed enhancement of MBE selectivity.

DRIFT Spectroscopy of CO Adsorption (DRIFT CO). Figure 9 shows the DRIFT spectra of adsorbed CO for the MN100 starting material and catalysts. Bands corresponding to terminal Pd-CO species are observed in the range 2000 to 2250 cm^{-1}.[28,29] The strong vibration is observed at 1900 cm^{-1} in all the materials and may be attributed to the HPS support, which overlaps with doubly and triply bridging carbonyls and prevents their observation.

As can be seen from Figure 9, after exposure to CO and purging with He, almost all the Pd catalysts (the exception is 0.7%-Pd/MN100-K-3-R) contain bands at 2165 and 2228 cm^{-1}, which can be attributed to formation of Pd^{2+} carbonyl species[29]). Interestingly, the Pd^{2+}-CO band is red-shifted to 2191 cm^{-1} for the sample 0.7%-Pd/MN100-K-3-R, suggesting the presence of carbonyls $Pd^{\delta+}$−CO[29] and a stronger Pd−K interaction induced by reductive treatment.[8]

Besides, in many cases two additional bands are observed at 2040 and 2076 cm^{-1} which may be attributed to CO adsorbing the Pd NPs or Pd(0) clusters.[24,28,30] Hence, some samples present both Pd(0) and Pd^{2+} sites. It is noteworthy that for the sample reduced with hydrogen directly in the DRIFT cell at a temperature of 300 °C, the existence of the band at 2040 cm^{-1} is likely due to the formation of bigger Pd NPs or clusters[24] in comparison with the neighboring band at 2076 cm^{-1}. This observation is in good agreement with the data of XPS and HAADF STEM study showing the formation of Pd NPs with higher mean diameter after the gas-phase reduction in H_2 flow at 300 °C in comparison with the *in situ* reduction.

4. CONCLUSIONS

The effect of alkali metal dopants (NaOH and KOH) on Pd NPs stabilized within hyper-cross-linked polystyrene (Pd/MN100 catalyst) used in the partial hydrogenation of MBY was studied. The addition of NaOH and KOH to the Pd/MN100 catalyst increases both the activity (ca. 1.7 times) and selectivity to MBE (up to ca. 99.5%) and reduces the reaction induction period. Characterization of the catalysts suggests that the alkali metal hydroxides at low concentrations facilitate the transformation of the Pd^{2+} residues into Pd(0), the latter being the active catalytic species. The alkali metal ions also increase the selectivity of the partial hydrogenation of MBY to MBE due to their presence on the Pd NPs surfaces as confirmed by HRTEM-EDX. K and Na may interact with the surface of PdNPs resulting in the so-called "site separation effect" which changes the adsorption of reactants. However, at high concentrations the alkali metal ions block the majority of catalytically active sites resulting in a significant decrease of activity.

■ ASSOCIATED CONTENT

Supporting Information

The Supporting Information is available free of charge on the ACS Publications website at DOI: 10.1021/acs.iecr.7b01612.

XPS spectra (including survey spectra and high resolution spectra of Pd 3d) of all the synthesized MN100-based catalysts as well as of the reference catalyst 1%-Pd/AC (PDF)

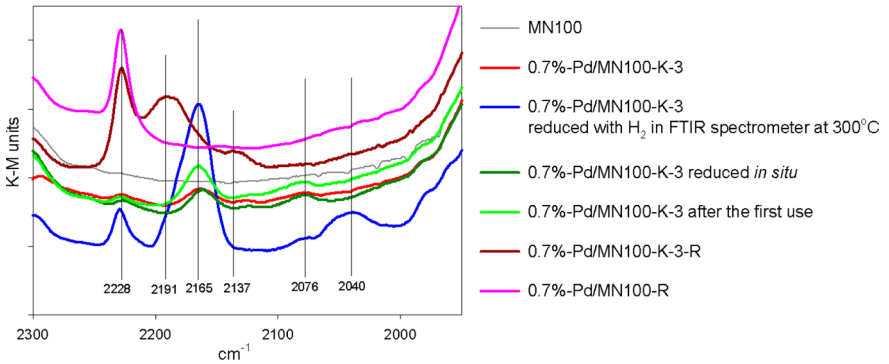

Figure 9. DRIFT spectra of adsorbed CO on the MN100 starting material and catalysts. IR spectra were recorded after exposure to CO at 10 °C for 5 min followed by treatment with He (100 mL/min, 10 °C, 10 min).

DOI: 10.1021/acs.iecr.7b01612
Ind. Eng. Chem. Res. XXXX, XXX, XXX−XXX

AUTHOR INFORMATION

Corresponding Authors

*E-mail: nlinda@science.tver.ru. Tel.; +74822789317.
*E-mail: Lioubov.kiwi-minsker@epfl.ch. Tel.: +41216933182.

ORCID

Jeremy S. Luterbacher: 0000-0002-0967-0583
Paul J. Dyson: 0000-0003-3117-3249
Lioubov Kiwi-Minsker: 0000-0002-7192-7212

Notes

The authors declare no competing financial interest.

ACKNOWLEDGMENTS

Financial support was provided by the Russian Science Foundation (Project 15-19-20023). We thank Ms. Ekaterina A. Kholkina (Tver Technical University, Tver, Russia) for help determining catalyst stability, and Mr. Oliver Anthony Beswick and Mr. Saeed Mohammadi Siyani (EPFL, Lausanne, Switzerland) for help with the HAADF STEM study.

REFERENCES

(1) Bonrath, W.; Medlock, J.; Schütz, J.; Wüstenberg, B.; Netscher, T. Hydrogenation in the Vitamins and Fine Chemicals Industry − An Overview. In *Hydrogenation*; Karamé, I., Ed.; InTech, 2012; pp 69−90.

(2) Bonrath, W.; Eggersdorfer, M.; Netscher, T. Catalysis in the Industrial Preparation of Vitamins and Nutraceuticals. *Catal. Today* **2007**, *121*, 45.

(3) Lindlar, H. Ein neuer Katalysator für selektive Hydrierungen. *Helv. Chim. Acta* **1952**, *35*, 446.

(4) Witte, P. T.; Berben, P. H.; Boland, S.; Boymans, E. H.; Vogt, D.; Geus, J. W.; Donkervoort, J. G. BASF NanoSelect Technology: Innovative Supported Pd- and Pt-based Catalysts for Selective Hydrogenation Reactions. *Top. Catal.* **2012**, *55*, 505.

(5) Kiwi-Minsker, L.; Crespo-Quesada, M. Shape and Size-Tailored Pd Nanocrystals to Study the Structure Sensitivity of 2-Methyl-3-butyn-2-ol Hydrogenation: Effect of the Stabilizing Agent. *Top. Catal.* **2012**, *55*, 486.

(6) Borodziński, A.; Bond, G. C. Selective Hydrogenation of Ethyne in Ethene-Rich Streams on Palladium Catalysts. Part 1. Effect of Changes to the Catalyst During Reaction. *Catal. Rev.: Sci. Eng.* **2006**, *48*, 91.

(7) Yarulin, A.; Yuranov, I.; Cardenas-Lizana, F.; Alexander, D. T. L.; Kiwi-Minsker, L. How to Increase the Selectivity of Pd-based Catalyst in Alkynol Hydrogenation: Effect of Second Metal. *Appl. Catal., A* **2014**, *478*, 186.

(8) Pellegrini, R.; Leofanti, G.; Agostini, G.; Bertinetti, L.; Bertarione, S.; Groppo, E.; Zecchina, A.; Lamberti, C. Influence of K-doping on a Pd/SiO_2-Al_2O_3 Catalyst. *J. Catal.* **2009**, *267*, 40.

(9) Jia, L.; Bulushev, D. A.; Beloshapkin, S.; Ross, J. R. H. Hydrogen Production from Formic Acid Vapour over a Pd/C Catalyst Promoted by Potassium Salts: Evidence for Participation of Buffer-like Solution in the Pores of the Catalyst. *Appl. Catal., B* **2014**, *160−161*, 35.

(10) Cho, H.-B.; Hong, B.-E.; Park, J.-H.; Ahn, S.-H.; Park, Y.-H. Effects of Catalyst Promotion on the Selective Hydrogenation of Biphenol Using Various Pd/C Catalysts. *Bull. Korean Chem. Soc.* **2008**, *29*, 2434.

(11) Zhang, W.; Zhu, Y.; Niu, S.; Li, Y. A Study of Furfural Decarbonylation on K-doped Pd/Al_2O_3 Catalysts. *J. Mol. Catal. A: Chem.* **2011**, *335*, 71.

(12) Aramendía, M. A.; Burch, R.; García, I. M.; Marinas, A.; Marinas, J. M.; Southward, B. W. L.; Urbano, F. J. The Effect of the Addition of Sodium Compounds in the Liquid-phase Hydrodechlorination of Chlorobenzene over Palladium Catalysts. *Appl. Catal., B* **2001**, *31*, 163.

(13) Aramendía, M. A.; Boráu, V.; García, I. M.; Jiménez, C.; Lafont, F.; Marinas, A.; Marinas, J. M.; Urbano, F. J. Liquid-phase Hydrodechlorination of Chlorobenzene over Palladium-supported Catalysts: Influence of HCl Formation and NaOH Addition. *J. Mol. Catal. A: Chem.* **2002**, *184*, 237.

(14) Moreno, J. M.; Aramendía, M. A.; Marinas, A.; Marinas, J. M.; Urbano, F. J. Hydrodechlorination of 3-Chloropyridine and Chlorobenzene in Methanol Solution over Alkali-modified Zirconia-Supported Palladium Catalysts. *Appl. Catal., B* **2005**, *59*, 275.

(15) Telkar, M. M.; Rode, C. V.; Rane, V. H.; Chaudhari, R. V. Influence of Alkali Metal Doping on Selectivity Behaviour of Platinum Catalysts for Hydrogenation of 2-Butyne-1,4-diol. *Catal. Commun.* **2005**, *6*, 725.

(16) Sabrowsky, H.; Bronger, W.; Schmitz, D. Z. Darstellung und Kristallstruktur von K_2PdO_2. *Z. Naturforsch., B: J. Chem. Sci.* **1974**, *29b*, 10.

(17) Nemygina, N. A.; Nikoshvili, L. Zh.; Matveeva, V. G.; Sulman, M. G.; Sulman, E. M.; Kiwi-Minsker, L. Pd-Nanoparticles Confined Within Hollow Polymeric Framework as Effective Catalysts for the Synthesis of Fine Chemicals. *Top. Catal.* **2016**, *59*, 1185.

(18) Nikoshvili, L.; Makarova, A. S.; Lyubimova, N. A.; Bykov, A. V.; Sidorov, A. I.; Tyamina, I. Yu.; Matveeva, V. G.; Sulman, E. M. Kinetic study of Selective Hydrogenation of 2-Methyl-3-butyn-2-ol over Pd-containing Hypercrosslinked Polystyrene. *Catal. Today* **2015**, *256*, 231.

(19) Nikoshvili, L.; Shimanskaya, E.; Bykov, A.; Yuranov, I.; Kiwi-Minsker, L.; Sulman, E. Selective Hydrogenation of 2-Methyl-3-butyn-2-ol over Pd-nanoparticles Stabilized in Hypercrosslinked Polystyrene: Solvent Effect. *Catal. Today* **2015**, *241* (B), 179.

(20) Sulman, E. M.; Nikoshvili, L.; Matveeva, V. G.; Tyamina, I.; Sidorov, A. I.; Bykov, A. V.; Demidenko, G. N.; Stein, B. D.; Bronstein, L. M. Palladium Containing Catalysts Based on Hypercrosslinked Polystyrene for Selective Hydrogenation of Acetylene Alcohols. *Top. Catal.* **2012**, *55*, 492.

(21) Lamy-Pitara, E.; El Mouahid, S.; Kerkeni, S.; Barbier, J. Effect of Anions and Cations on the Aqueous Phase Catalytic Hydrogenation of C═C Bonds. *Electrochim. Acta* **2003**, *48*, 4311.

(22) Gravelle-Rumeau-Maillot, M.; Pitchon, V.; Martin, G. A.; Praliaud, H. Complementary Study by Calorimetry and Infrared Spectroscopy of Alkali Metal Doped Pd/SiO_2 Solids: Adsorption of Hydrogen and Carbon Monoxide. *Appl. Catal., A* **1993**, *98*, 45.

(23) Protasova, L. N.; Rebrov, E. V.; Choy, K. L.; Pung, S. Y.; Engels, V.; Cabaj, M.; Wheatley, A. E. H.; Schouten, J. C. ZnO Based Nanowires Grown by Chemical Vapour Deposition for Selective Hydrogenation of Acetylene Alcohols. *Catal. Sci. Technol.* **2011**, *1*, 768.

(24) Wagner, C. D.; Rigs, W. M. *Handbook of X-ray Photoelectron Spectroscopy*, Perkin-Elmer Corporation, 1979. NIST X-ray Photoelectron Spectroscopy Database, version 4.1 National Institute of Standards and Technology: Gaithersburg, MD, 2012.

(25) Wu, T.; Kaden, W. E.; Kunkel, W. A.; Anderson, S. L. Size-dependent Oxidation of Pd_n ($n \leq 13$) on Alumina/NiAl(110): Correlation with Pd Core Level Binding Energies. *Surf. Sci.* **2009**, *603*, 2764.

(26) Paredis, K.; Ono, L. K.; Behafarid, F.; Zhang, Z.; Yang, J. C.; Frenkel, A. I.; Cuenya, B. R. Evolution of the Structure and Chemical State of Pd Nanoparticles during the in Situ Catalytic Reduction of NO with H_2. *J. Am. Chem. Soc.* **2011**, *133*, 13455.

(27) Nemygina, N. A.; Nikoshvili, L.; Bykov, A. V.; Sidorov, A. I.; Molchanov, V. P.; Sulman, M. G.; Tiamina, I.; Stein, B. D.; Matveeva, V. G.; Sulman, E. M.; Kiwi-Minsker, L. Catalysts of Suzuki Cross-Coupling Based on Functionalized Hyper-cross-linked Polystyrene: Influence of Precursor Nature. *Org. Process Res. Dev.* **2016**, *20*, 1453.

(28) Groppo, E.; Agostini, G.; Borfecchia, E.; Wei, L.; Giannici, F.; Portale, G.; Longo, A.; Lamberti, C. Formation and Growth of Pd Nanoparticles Inside a Highly Cross-Linked Polystyrene Support: Role of the Reducing Agent. *J. Phys. Chem. C* **2014**, *118*, 8406.

(29) Hadjiivanov, K. I.; Vayssilov, G. N. Characterization of Oxide Surfaces and Zeolites by Carbon Monoxide as an IR Probe Molecule. *Adv. Catal.* **2002**, *47*, 307.

(30) Yudanov, I. V.; Sahnoun, R.; Neyman, K. M.; Rösch, N.; Hoffmann, J.; Schauermann, S.; Johanek, V.; Unterhalt, H.; Rupprechter, G.; Libuda, J.; Freund, H.-J. CO Adsorption on Pd

DOI: 10.1021/acs.iecr.7b01612
Ind. Eng. Chem. Res. XXXX, XXX, XXX−XXX

Nanoparticles: Density Functional and Vibrational Spectroscopy Studies. *J. Phys. Chem. B* **2003**, *107*, 255.

DOI: 10.1021/acs.iecr.7b01612
Ind. Eng. Chem. Res. XXXX, XXX, XXX−XXX